Universal Decay of the Classical Loschmidt Echo of Neutrally Stable Mixing Dynamics

Giulio Casati,[1,2,3] Tomaž Prosen,[4,3] Jinghua Lan,[3] and Baowen Li[3]

[1]*Center for Nonlinear and Complex Systems, Università degli studi dell'Insubria, Como, Italy*
[2]*Istituto Nazionale di Fisica della Materia, Unità di Como, and Istituto Nazionale di Fisica Nucleare, Sezione di Milano, Milano, Italy*
[3]*Department of Physics, National University of Singapore, Singapore 117542, Republic of Singapore*
[4]*Physics Department, Faculty of Mathematics and Physics, University of Ljubljana, Ljubljana, Slovenia*

(Received 5 October 2004; published 21 March 2005)

We provide analytical and numerical evidence that the classical mixing systems, which lack exponential sensitivity on initial conditions, exhibit universal decay of the Loschmidt echo which turns out to be a function of a single scaled time variable $\delta^{2/5}t$, where δ is the strength of perturbation. The role of dynamical instability and entropy production is discussed.

DOI: 10.1103/PhysRevLett.94.114101 PACS numbers: 05.45.Mt, 03.67.Lx, 05.45.Ac

Fidelity, or Loschmidt echo, is defined as the overlap of two time evolving states which, starting from the same initial condition, evolve under two slightly different Hamiltonians. It is therefore an important quantity which measures the stability of the motion under systems perturbations. The recent interest in the behavior of fidelity [1–11] has been largely motivated by a possible use in quantifying stability of quantum computation [12].

It has been shown [10] that for classical chaotic, exponentially unstable systems, the decay rate of fidelity is *perturbation independent* and, asymptotically, fidelity decays as correlation functions. On the other hand, for quantum systems, fidelity decay obeys different regimes *depending* on perturbation strength. In this relation, particularly intriguing is the recently discovered case of mixing dynamics with vanishing Lyapounov exponent [13,14] a prominent example of which are billiards inside polygons [15]. In several respects the classical dynamics of such systems is reminiscent of quantum dynamics of generic chaotic systems which, apart from an initial time, logarithmically short in $\hbar$, are linearly stable. As a consequence statistical relaxation in quantum mechanics takes place in the absence of exponential instability. Certainly, the dramatic difference in the dynamical stability properties of different systems must be reflected in a different qualitative behavior of physical quantities such as fidelity which is the object of the present Letter.

In the following, under the assumptions of linear separation of trajectories and dynamical mixing, which may be produced by some discontinuity in the flow, we derive a universal scaling law of classical fidelity decay. We conjecture that this surprising fidelity decay may be associated to the power-logarithmic entropy production in such systems. We consider here a specific example, i.e., the triangle map $z_{n+1} = T(z_n)$ [14] on a torus $z = (x, y) \in [-1, 1) \times [-1, 1)$,

$$\begin{aligned} y_{n+1} &= y_n + \alpha\,\mathrm{sgn}x_n + \beta \pmod 2, \\ x_{n+1} &= x_n + y_{n+1} \pmod 2, \end{aligned} \tag{1}$$

where $\mathrm{sgn}x = \pm 1$ is the sign of x and α, β are two parameters. Previous investigations have shown that [14] [see also [16] for some rigorous results on (1)] for rational values of α, β the system is pseudointegrable, as the dynamics is confined on invariant curves. If $\alpha = 0$ and β is irrational, the dynamics is (uniquely) ergodic, but not mixing, while for incommensurate irrational values of α, β the dynamics is ergodic and mixing with dynamical correlation functions decaying as $t^{-3/2}$. It can be argued that the triangle map possesses the essential features of bounce maps of polygonal billiards and 1D hardpoint gases [13,14], namely, parabolic stability in combination with decaying dynamical correlations and as such represents a paradigmatic model for a larger class of systems.

The classical fidelity $F_\delta(n)$ can be written as an overlap of two phase-space densities propagated by the original map T and the perturbed map $T_\delta = T \circ g_\delta$, where $g_\delta(z) = z + \delta a(z)$ is some near-identity area-preserving map parametrized by a vector field $a(z)$:

$$F_\delta(n) = \frac{\int d^2z \rho(T^{(-n)}(z))\rho(T_\delta^{(-n)}(z))}{\int d^2z \rho^2(z)}. \tag{2}$$

We can make our discussion even more general by taking the perturbation *explicitly time dependent*. Let the perturbed map $T_{\delta,n}$ explicitly depend on iteration time; namely, we consider the following class of perturbed triangle maps, $\bar{z}_{n+1} = T_{\delta,n}(\bar{z}_n)$:

$$\begin{aligned} \bar{y}_{n+1} &= \bar{y}_n + \alpha\,\mathrm{sgn}\bar{x}_n + \beta + \delta f_n(\bar{x}_n) \pmod 2, \\ \bar{x}_{n+1} &= \bar{x}_n + \bar{y}_{n+1} \pmod 2. \end{aligned} \tag{3}$$

We assume that the *force function* f_n has a *vanishing time average* for almost any initial condition. Let us further assume that the initial density $\rho(z)$ is a characteristic function over some set $\mathcal{A}$ of typical diameter ω with $\delta \ll \omega \ll 1$. Then a pair of orbits z_n and $\bar{z}_n$ starting from the same point $\bar{z}_0 = z_0$ in $\mathcal{A}$ contribute to (2) until they hit the opposite sides of the discontinuity, at $x = 0, 1 \pmod 2$. The fidelity at time n is then simply the probability that

the shortest line between the pair of orbits does not hit the cut up to the nth iterate. Assuming ergodicity of the map [14] we write

$$F_\delta(n) = \left\langle \prod_{n'=1}^{n} (1 - |\Delta x_{n'}|) \right\rangle \tag{4}$$

where $\Delta x_n = \bar{x}_n - x_n$, and $\langle A_n \rangle = \int dz \rho(z) A(T^{(n)}(z))/\int dz \rho(z)$. In order to derive the fidelity decay for the triangle map we have to compute the average growth rate of the orbits' distance perpendicular to the cut. This is achieved by writing out an explicit linearized map for the orbits' displacement $\Delta z_n = \bar{z}_n - z_n$,

$$\Delta z_{n+1} = \begin{pmatrix} 1 & 1 \\ 0 & 1 \end{pmatrix} \Delta z_n + \begin{pmatrix} 1 \\ 1 \end{pmatrix} \delta f_n(x_n). \tag{5}$$

This system of linear difference equations can be solved explicitly, say for Δx_n,

$$\Delta x_n = \delta \sum_{n'=0}^{n-1} (n - n') f_{n'}(x_{n'}) \tag{6}$$

with the initial condition $\Delta z_0 = 0$. Assuming that f_n are pseudorandom variables with quickly decaying correlation function $C(n) = \lim_{m\to\infty} \langle f_m(x_m) f_{n+m}(x_{n+m}) \rangle$, we can employ a version of the *central limit theorem* to show that Δx_n should have *Gaussian distribution* for sufficiently large n. To this end, let us first notice that the second moment

$$\langle (\Delta x_n)^2 \rangle = \delta^2 \sum_{n'=0}^{n-1} \sum_{n''=0}^{n-1} (n - n')(n - n'') \langle f_{n'} f_{n''} \rangle \tag{7}$$

can be related, as $n \to \infty$, to the integrated correlation function. Since, for large n', n'', $\langle f_{n'} f_{n''} \rangle = C(n' - n'')$, we obtain by means of a straightforward calculation

$$\langle (\Delta x_n)^2 \rangle \to \frac{1}{3} \delta^2 n^3 \sigma, \qquad \sigma := \sum_{m=-\infty}^{\infty} C(m). \tag{8}$$

Now, as long as fidelity remains close to 1, we can expand (4) to first order $F_\delta(n) = 1 - \sum_{n'=1}^{n} \langle |\Delta x_{n'}| \rangle$, where the average $\langle |\Delta x_n| \rangle = \sqrt{2\sigma/(3\pi)} |\delta| |n|^{3/2}$ can be computed using a Gaussian distribution of Δx_n with variance $\langle (\Delta x_n)^2 \rangle$ given in (8). This yields

$$F_\delta(n) = 1 - \sqrt{\frac{8\sigma}{75\pi}} |\delta| |n|^{5/2}. \tag{9}$$

This expression is valid until $F_\delta(n)$ remains close to 1, that is, up to time $|n| < n^* = \sigma^{-1/5} |\delta|^{-2/5}$.

In Fig. 1(a) we show the behavior of $1 - F_\delta(n)$ for short times $n < n^*$ and compare with the theoretical formula (9) with $\sigma = 3.29 \pm 0.01$ as computed from the numerical simulation of the correlation function $C(n)$. As for perturbation we choose a simple shift in the parameter α, so the force reads $f(x) = \mathrm{sgn} x$ and is, in this case, *not explicitly* time dependent. Yet it is pseudorandom and one can see

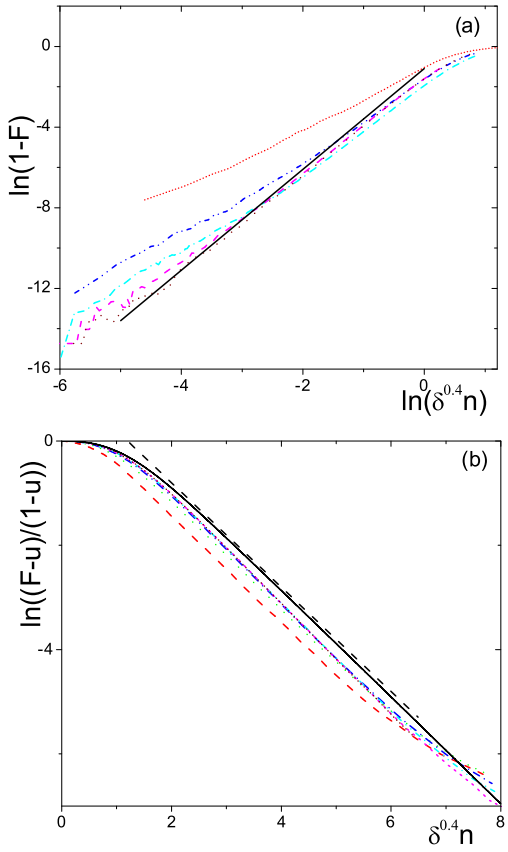

FIG. 1 (color online). Fidelity decay. To compute fidelity we divide the phase space in 100×100 cells. We then take 10^5 points in one cell and evolve these points with the map (1) up to time n. Then we compute the reverse evolution with the map (3) and compute the fraction of points which fall again in the initial cell, after time $2n$. The result is then averaged over initial distributions in 49 different randomly chosen cells. (a) $\log[1 - F_\delta(n)]$ versus $\log(\delta^{2/5} n)$ magnifying the behavior for short times. The broken curves refer to $\delta = 10^{-5}, \ldots, 10^{-10}$ (from top to bottom). The full line is the theoretical expression (9). (b) $\log[(F_\delta(n) - u)/(1 - u)]$ versus $\delta^{2/5} n$ magnifying asymptotic (long-time) behavior. Here $u = 10^{-4}$ is the relative area of the initial set $\mathcal{A}$ giving the asymptotic value of fidelity. The meaning of broken curves is the same as in (a). The full curve gives the numerical solution of the random Gaussian model (12), while the dashed line has slope -1 to indicate asymptotic exponential decay.

that, as δ decreases, the numerical curves approach the theoretical expression (9).

Notice that according to Eq. (8), the average distance between two orbits increases as $\propto n^{3/2}$. On the other hand, the distance between two initially close orbits of the *same* map increases only linearly with time. This is nicely confirmed by the numerical simulations of Fig. 2.

For larger times, $n > n^*$, higher order terms in the expansion of (4) contribute, so temporal correlations among Δx_n become important. We are here unable to derive the exact theoretical predictions for the fidelity

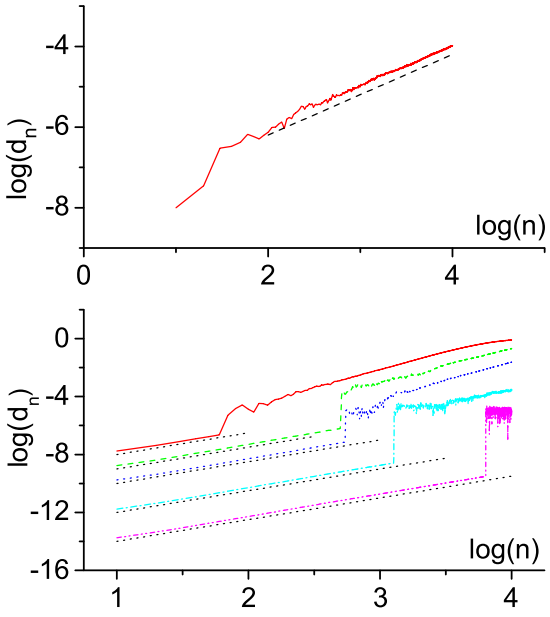

FIG. 2 (color online). (a) Average distance $d_n = |\Delta z_n|$ versus time n for two nearby initial orbits of the unperturbed map (1). The initial distance is $d_0 = 10^{-9}$; the average is taken over 2.5×10^8 different initial conditions. The dotted line has slope 1. (b) Average distance versus time for two orbits starting from the same initial condition and evolving under the unperturbed and perturbed maps, (1) and (3), respectively. The values of perturbation δ, for the curves (from top to bottom), are 10^{-9}, 10^{-10}, 10^{-11}, 10^{-13}, and 10^{-15}. The data are averaged over 10^5 different initial conditions. The dotted lines have slope 1.5.

decay in this regime. However, numerical results in Fig. 1(b) show that, for large times, fidelity decays exponentially $F_\delta(n) = \exp(-\gamma|n|)$ with exponent $\gamma = C|\delta|^{2/5}$. We also checked that the transition time between the two regimes of decay scales as $\delta^{-2/5}$. In conclusion, extensive and accurate numerical results provide clear evidence that fidelity depends on the single scaling variable $\tau = |\delta|^{2/5}n$.

In the following, we show that this scaling behavior can be derived analytically for sufficiently small δ. The only assumption is correlation decay with a *finite* characteristic time scale $n_{\rm mix}$; i.e., $\langle f_n f_{n'}\rangle$ practically vanish for $|n - n'| > n_{\rm mix}$. Let us divide the time span n into $\nu := n/m$ blocks of m steps each, such that $n_{\rm mix} \ll m \ll n$, and make a scaling argument. The local variation of Δx_n, namely, $\Delta x_{n+1} - \Delta x_n = \delta \sum_{n'=0}^{n} f_{n'} \sim \delta\sqrt{n}$ is much smaller than the mean value $\langle|\Delta x_n|\rangle \sim \delta n^{3/2}$. Thus we approximate the product (4) within each block labeled by $\iota = 1, \ldots, \nu$ as $(1 - |\Delta x_{(\iota-1)m}|)^m \approx 1 - m|\Delta x_{(\iota-1)m}|$. Therefore

$$F_\delta(n) \approx \prod_{\iota=1}^{\nu}(1 - m|\Delta x_{(\iota-1)m}|). \tag{10}$$

Next we define the normalized block-averaged forces

$$\xi_\iota = \frac{1}{\sqrt{\sigma m}} \sum_{k=0}^{m-1} f_{(\iota-1)m+k} \tag{11}$$

which are normalized, and uncorrelated, $\langle \xi_\iota \xi_\mu\rangle = \delta_{\iota\mu}$ since $m \gg n_{\rm mix}$. Using Eq. (6) we can write $\Delta x_{(\iota-1)m} \approx \delta \sum_{\mu=1}^{\iota}(\iota - \mu)m \sum_{k=0}^{m-1} f_{(\mu-1)m+k} = \delta m^{3/2}\sigma^{1/2} \times \sum_{\mu=1}^{\iota}(\iota - \mu)\xi_\mu$. If, in addition to the rescaled time $\nu = n/m$, we define a rescaled perturbation $\epsilon = \delta\sigma^{1/2}m^{5/2}$ then we can write Eq. (10) as

$$\Phi_\epsilon(\nu) = \left\langle \prod_{\iota=1}^{\nu}\left(1 - \left|\epsilon \sum_{\mu=0}^{\iota-1}(\iota - \mu)\xi_\mu\right|\right)\right\rangle_\xi . \tag{12}$$

The derived relation $F_\delta(n) = \Phi_{\delta\sigma^{1/2}m^{5/2}}(n/m)$ does not depend on m (for large enough m), and therefore fidelity should be a function of the scaling variable $\tau = |\delta|^{2/5}n$ only.

Notice that due to the central limit theorem, since $m \gg n_{\rm mix}$, ξ_μ can be simply treated as uncorrelated, normalized, Gaussian stochastic variables. We have actually computed the *universal function* $\phi(\epsilon^{2/5}\nu) = \Phi_\epsilon(\nu)$ by means of Monte Carlo integration and checked that it is practically insensitive to ϵ, for $\epsilon < 10^{-4}$. As is seen in Fig. 1(b), the numerical data for the triangle map agree with the theoretical expression (12), namely, $\phi(\delta^{2/5}\sigma^{1/5}n)$ which is plotted as a full curve.

The two regimes of fidelity decay described above are illustrated in Fig. 3 by the image at the echo time of an initial uniform phase-space distribution over some set $\mathcal{A}$.

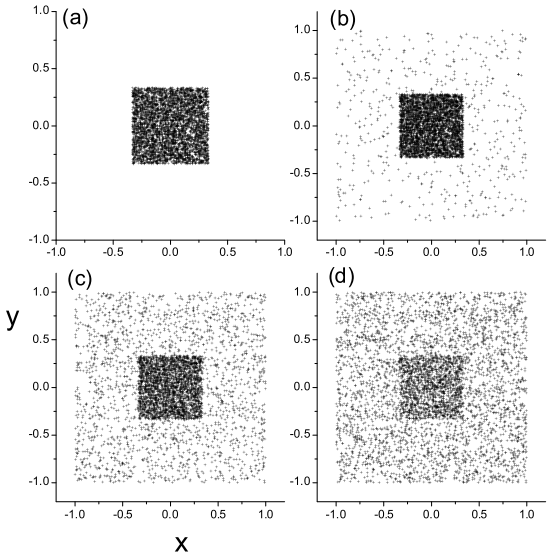

FIG. 3. Spreading of phase-space points of the echo dynamics. We consider 5000 initial points in the central cell of a 3×3 grid (a). We then evolve these points up to time n and then reverse the motion with the perturbed dynamics, with $\delta = 10^{-6}$, up to the echo time $2n$. The density of points, for $n = 200$, 400, 600 is shown in (b),(c),(d), respectively.

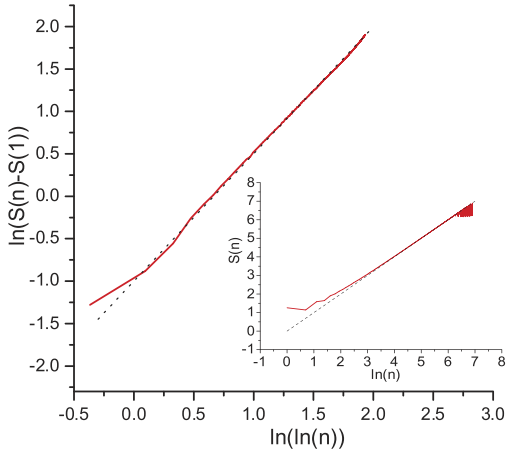

FIG. 4 (color online). The time evolution of the coarse-grained entropy for the triangle map, computed by taking 5×10^7 points initially distributed randomly in one cell of a $N \times N$ phase-space grid with $N = 700$. We plot $\ln[S(n) - S(1)]$ versus $\ln \ln n$. The straight line has slope $3/2$. Obviously, the entropy will eventually saturate at $S(\infty) = \ln N^2$. In the inset we show the entropy computed for the uniquely ergodic and nonmixing dynamics with $\alpha = 0$. The dotted line has slope 1.

Notice that the linear-response regime (9) is valid until the shape of the initial set is approximately restored at the echo time. For larger times, the fidelity decay becomes exponential.

Finally we stress that this behavior of the triangle map differs from the typical behavior which has been found for chaotic or for integrable systems. In particular, contrary to the case of exponentially unstable systems, in this case the rate of fidelity decay depends on the perturbation strength. This feature is shared by quantum systems in which exponential instability is absent as well. One may wonder if this behavior is reflected also in some other, perhaps even more fundamental dynamical property of the map. In order to explore this question, we have computed the entropy production for the map (1). As the extensive computation of Kolmogorov-Sinai dynamical entropies seemed too expensive for reaching any conclusive results, we have decided to compute the dynamical evolution of the coarse-grained statistical entropy $S_n = -\sum_j p_n^{(j)} \ln p_n^{(j)}$. To this end we divide the phase space in $N \times N$ equal cells and consider an initial ensemble of points uniformly distributed over one cell. The probability $p_n^{(j)}$ is defined as the fraction of orbits which, after n time steps, fall in the cell of label j. For a chaotic system with dynamical entropy h, one expects $S_n = hn + \text{const}$ [17], whereas for ergodic-only (nonmixing) dynamics one expects $S_n \sim \ln n$, for sufficiently large N. Our numerical results for the triangle map (Fig. 4) show instead that $S_n - S_1 = |\ln n|^\lambda$ with the exponent $\lambda = 3/2$. Furthermore, as shown in the inset of Fig. 4, for the triangle map (1) with $\alpha = 0$ numerical results give, quite accurately, $S(n) = \ln n$ (with no prefactor or additional constant).

In conclusion, we have discussed the parametric stability, as characterized by classical fidelity or Loschmidt echo, of an important class of dynamical systems where neutral stability is coexisting with dynamical mixing. As a paradigmatic example of this class of systems we have considered the triangle map. By means of analytic calculations and numerical simulations we have derived two universal regimes of fidelity decay, both being characterized by a universal scaled time variable $|\delta|^{2/5}t$. This interesting dynamical behavior is supported also by a power-logarithmic behavior of the coarse-grained entropy.

We acknowledge financial support by the PRIN 2002 "Fault tolerance, control and stability of quantum information processing" and PA INFM "Weak chaos: Theory and applications" (G. C.), by Grant No. P1-044 of Ministry of Education, Science and Sport of Slovenia (T. P.), by Grant No. DAAD19-02-1-0086, ARO United States (G. C. and T. P.), by the Faculty Research Grant of NUS, and by DSTA, Singapore, under Project Agreement No. POD0410553 (B. L.).

[1] A. Peres, Phys. Rev. A **30**, 1610 (1984).
[2] H. M. Pastawski *et al.*, Physica (Amsterdam) **283A**, 166 (2000).
[3] R. A. Jalabert and H. M. Pastawski, Phys. Rev. Lett. **86**, 2490 (2001).
[4] T. Prosen, Phys. Rev. E **65**, 036208 (2002).
[5] Ph. Jacquod *et al.*, Phys. Rev. E **64**, 055203(R) (2001).
[6] N. R. Cerruti and S. Tomsovic, Phys. Rev. Lett. **88**, 054103 (2002).
[7] G. Benenti and G. Casati, Phys. Rev. E **65**, 066205 (2002).
[8] T. Prosen and M. Žnidarič, J. Phys. A **35**, 1455 (2002).
[9] B. Eckhardt, J. Phys. A **36**, 371 (2003).
[10] G. Benenti, G. Casati, and G. Veble, Phys. Rev. E **67**, 055202 (2003).
[11] G. Veble and T. Prosen, Phys. Rev. Lett. **92**, 034101 (2004).
[12] G. Benenti, G. Casati, and G. Strini, *Basic Concepts*, Principles of Quantum Computation and Information Vol. I (World Scientific, Singapore, 2004); M. A. Nielsen and I. L. Chuang, *Quantum Computation and Quantum Information* (Cambridge University Press, Cambridge, 2001).
[13] G. Casati and T. Prosen, Phys. Rev. Lett. **83**, 4729 (1999).
[14] G. Casati and T. Prosen, Phys. Rev. Lett. **85**, 4261 (2000).
[15] Strictly speaking there is no rigorous proof that irrational polygons are mixing. We refer here to the evidence provided by numerical computations such as those reported in Refs. [13,14].
[16] M. Degli Esposti and S. Galatolo, report, http://www.dm.unibo.it/fismat/pub/CPco010404.pdf
[17] V. Latora and M. Baranger, Phys. Rev. Lett. **82**, 520 (1999).